Egyptian Chinese Journal Of Applied Science

Volume 1, Issue 1 — June 2025

A Theoretical Exploration of Gravity Effects on Micro-Elongated Thermoelastic Media in Infinite Inviscid Fluids

Mohamed.F. Ismail[1*], Hazem Elsadek[1]

[1] Faculty of Computers and Information System, Egyptian Chinese University, Cairo, Egypt.

[*] Corresponding author: Mohamed.Fekry.ecu.edu.eg

Abstract:

This study presents a thorough examination of the dynamic response of a micro-elongated thermoelastic half-space immersed in an unbounded, non-viscous fluid, with particular attention given to the influence of gravity. The investigation is conducted using two distinct thermoelastic frameworks: the Lord-Shulman (L-S) model and the Dual-Phase-Lag (DPL) model. The governing equations are meticulously derived according to each theoretical model. An analytical solution is achieved through the use of the normal mode analysis method. Aluminum epoxy is selected as the representative material to demonstrate and compare how gravity affects the interaction between the micro-elongated thermoelastic medium and the surrounding fluid. The findings obtained from the L-S model are directly compared with those from the DPL model to reveal variations in material behavior. The analysis clearly shows that gravity significantly impacts all considered physical quantities, including displacement, temperature, micro-elongation, and stress components.

Keywords: thermoelasticity, normal mode, gravity, micro-elongation.

1. Introduction:

Generalized thermoelasticity theories were developed to resolve the inconsistency arising from the assumption of infinite heat propagation speed inherent in classical coupled thermoelasticity, which is based on Fourier's parabolic heat conduction law as formulated by Biot [1]. To address this, Lord and Shulman [2] introduced a generalized thermoelastic model incorporating a single relaxation time. Subsequently, Green and Lindsay [3] proposed a version featuring two distinct relaxation times. Green and Naghdi [4–6] further advanced the field by formulating three additional models—commonly labeled as GN-I, GN-II, and GN-III. Of these, the linearized GN-I model aligns with classical thermoelastic theory. In contrast, GN-II assumes zero internal entropy production and no thermal energy dissipation, thus supporting the existence of undamped thermoelastic waves within the material. Othman [7] explored the combined impact of laser pulses and gravitational fields on thermoelastic media under the Green-Naghdi framework. Later, in 2012, Othman and Atwa [8] examined the deformation behavior of a micropolar thermoelastic solid with voids, considering various surface sources. Tzou [9,10] introduced the Dual-Phase-Lag (DPL) model, a novel approach to thermal transport that modifies Fourier's law by introducing two distinct time delays—one for heat flux and another for temperature gradient. Using the DPL model, Othman and Eraki [11] investigated the influence of gravity on thermoelastic diffusion triggered by laser pulses. The concept that solid materials can undergo both macro-deformations and micro-rotations was introduced by Eringen [12–14] through his linear theory of micropolar elasticity, which he later extended to thermo-microstretch elastic solids [15].

In micro-elongated elastic solids, four degrees of freedom exist: three for translational motion and one for micro-elongation. Beyond classical deformation, these materials allow for volumetric micro-elongation, where material particles can expand or contract independently of their translational motion. Examples of such media include solid-liquid crystals, composites reinforced with chopped elastic fibers, and porous materials saturated with inviscid fluids or gases. Shaw and Mukhopadhyay [16] analyzed the thermal response of a functionally graded, isotropic, unbounded micro-elongated medium under a periodically varying heat source. In another study [17], they examined thermoelastic interactions in a homogeneous, isotropic micro-elongated medium influenced by a moving heat source. Ailawalia and Sachdeva [18] investigated deformation caused by internal heat sources in a thermoelastic micro-elongated solid covered by an elastic layer of thickness hhh. Further, Sachdeva [19] studied two-dimensional deformation in such a medium interacting with a fluid layer. Ailawalia and Pathania [20] explored the effects of internal heat sources in a micro-elongated thermoelastic solid topped by an infinite elastic layer. Othman [21] employed the DPL model to assess the combined effects of gravitational fields and rotation on a generalized thermoelastic medium, while Ahmed [22] analyzed the influence of gravity on piezo-thermoelastic behavior within the DPL framework.

In the current study, we focus on examining the thermoelastic behavior of a micro-elongated half-space embedded in an infinitely extended, inviscid (non-viscous) fluid medium, while accounting for the effects of gravity, as schematically depicted in Fig. 1. The investigation is carried out using two primary theoretical frameworks: the Dual-Phase-Lag (DPL) model and the Lord–Shulman (L-

S) theory. The study begins with the systematic derivation and formulation of the governing equations that describe the physical behavior of the system under the specified conditions. To streamline the mathematical complexity and ensure dimensional consistency, a non-dimensionalization process is implemented, transforming the governing equations into a dimensionless form. This approach not only enhances the generality of the results but also simplifies the computational process. For analytical tractability, the normal mode analysis method is employed, which converts the system of partial differential equations (PDEs) into a set of ordinary differential equations (ODEs), making the problem more manageable within the given geometrical setup. Appropriate boundary conditions are then defined and imposed at the interface between the solid and fluid media. These conditions are crucial for determining the constants of integration that appear in the general solutions of the differential equations. By applying the boundary conditions rigorously, a complete and physically consistent solution is obtained. Finally, the theoretical outcomes are validated through numerical simulations. Detailed numerical calculations are performed to explore the physical consequences of incorporating gravity into the models. The resulting data are thoroughly analyzed, discussed, and presented through graphical illustrations to clearly demonstrate the impact of gravity on the various thermoelastic and microstructural fields within the medium.

2. Basic equations

The system of governing equations of a micro-elongated thermoelasticity with gravity in a dual-phase-lag model can be written as [18]

$$\sigma_{ij,j} = \rho u_{i,tt}, \tag{1}$$

$$a_0 \varphi_{,ii} + \beta_1 T - \lambda_1 \varphi - \lambda_0 u_{j,j} = \frac{1}{2} \rho j_0 \varphi_{,tt}, \tag{2}$$

$$k(1+\tau_\theta \frac{\partial}{\partial t}) T_{,ii} = (1+\tau_q \frac{\partial}{\partial t})(\rho c_e \frac{\partial T}{\partial t} + \beta_0 T u_{k,kt}) + \beta_1 T_0 \varphi_{,t}, \tag{3}$$

$$\sigma_{ij} = 2\mu \varepsilon_{ij} + (\lambda e - \beta_0 T + \lambda_0 \varphi)\delta_{ij}. \tag{4}$$

From equation (1) and equation (4) for displacement vector $\boldsymbol{u}(x,z,t) = u(u_1, 0, u_3)$ and the gravity g the equations of motion are given by [21-22]

$$\mu \nabla^2 u_1 + (\lambda+\mu) e_{,x} - \beta_0 T_{,x} + \lambda_0 \varphi_{,x} + \rho g \frac{\partial u_3}{\partial x} = \rho u_{1,tt}, \tag{5}$$

$$\mu \nabla^2 u_3 + (\lambda+\mu) e_{,z} - \beta_0 T_{,z} + \lambda_0 \varphi_{,z} - \rho g \frac{\partial u_1}{\partial x} = \rho u_{3,tt}. \tag{6}$$

For simplicity, the following non-dimensional variables are used

$$x_i' = \frac{w^*}{c_1} x_i, \quad z' = \frac{w^*}{c_1} z, \quad u_i' = \frac{w^* \rho c_1}{\beta_0 T_0} u_i, \quad u_i^{e'} = \frac{w^* \rho c_1}{\beta_0 T_0} u_i^e, \quad t' = w^* t, \quad \tau_\theta' = w^* \tau_\theta, \quad \tau_q' = w^* \tau_q,$$

$$\sigma_{ij}' = \frac{\sigma_{ij}}{\beta_0 T_0}, \; \sigma_{ij}^{e'} = \frac{\sigma_{ij}^e}{\beta_0 T_0}, \; \varphi' = \frac{\lambda_0}{\beta_0 T_0} \varphi, \; T' = \frac{T}{T_0}, \; g' = \frac{g}{w^* c_1}, \; P_1' = \frac{P_1}{\beta_0 T_0}, \tag{7}$$

Where, $\quad w^* = \dfrac{\rho c_1^2 c_e}{k}, \quad c_1^2 = \dfrac{\lambda + 2\mu}{\rho}.$

Substituting from Eqs. (7) into Eqs. (2), (3), (5), and (6), we obtain

$$a_1 \nabla^2 u_1 + a_2 e_{,x} - T_{,x} + \varphi_{,x} + g u_{3,x} = u_{1,tt}, \tag{8}$$

$$a_1 \nabla^2 u_3 + a_2 e_{,z} - T_{,z} + \varphi_{,z} - g u_{1,x} = u_{3,tt}, \tag{9}$$

$$(\nabla^2 - a_4)\varphi + a_3 T - a_5 e = a_6 \varphi_{,tt}, \tag{10}$$

$$(1+\tau_\theta \frac{\partial}{\partial t})\nabla^2 T = (1+\tau_q \frac{\partial}{\partial t})[a_7 T_{,t} + a_8 e_{,t}] + a_9 \varphi_{,t}. \tag{11}$$

3. Normal mode analysis

The solution of the physical variable recognized may be analysed in normal modes as the following form:

$$[u_i, \varphi, T, \sigma_{ij}, u_i^e, \sigma_{ij}^e](x,z,t) = [u_i^*, \varphi^*, T^*, \sigma_{ij}^*, u_i^{e*}, \sigma_{ij}^{e*}](z) e^{(wt+ibx)}. \tag{12}$$

Where w is a complex constant, $i = \sqrt{-1}$, b is wave number in the x direction.

Using Eq. (12) into Eqs. (8)-(11), then we have

$$[a_1 D^2 - \delta_1] u_1^* + [\delta_2 D + i b g] u_3^* - i b T^* + i b \varphi^* = 0, \tag{13}$$

$$[\delta_2 D - i b g] u_1^* + [\delta_3 D^2 - \delta_4] u_3^* - D T^* + D \varphi^* = 0, \tag{14}$$

$$-\delta_5 u_1^* - a_5 D u_3^* + a_3 T^* + [D^2 - \delta_6] \varphi^* = 0, \tag{15}$$

$$\delta_9 u_1^* + \delta_{10} D u_3^* + [-\delta_7 D^2 + \delta_{11}] T^* + \delta_{12} \varphi^* = 0. \tag{16}$$

Eqs. (13)-(16) have a non-trivial solution if the physical quantities' determinant coefficients equal to zero, then we get.

$$(\mathrm{D}^8 - A\mathrm{D}^6 + B\mathrm{D}^4 - C\mathrm{D}^2 + E)\{u_1^*(z), u_3^*(z), T^*(z), \varphi^*(z)\} = 0. \quad (17)$$

Eq. (18) can be factorized as:

$$(\mathrm{D}^2 - k_1^2)(\mathrm{D}^2 - k_2^2)(\mathrm{D}^2 - k_3^2)(\mathrm{D}^2 - k_4^2)\{u_1^*(z), u_3^*(z), T^*(z), \varphi^*(z)\} = 0. \quad (18)$$

Where, $k_n^2, (n = 1, 2, 3, 4)$ are roots of the characteristic equation of (18)

The general solutions of Eq. (18) bound as $(z \to \infty)$ is given by

$$(u_1^*, u_3^*, T^*, \varphi^*)(z) = \sum_{n=1}^{4}(1, H_{1n}, H_{2n}, H_{3n}) M_n e^{k_n z} + \sum_{n=1}^{4}(1, H_{1(n+4)}, H_{2(n+4)}, H_{3(n+4)}) M_{(n+4)} e^{-k_n z}. \quad (19)$$

Substituting from Eq. (7) into (4), and with the help of Eq. (19), we obtain the components of stresses.

$$(\sigma_{xx}, \sigma_{zz})(z) = \sum_{n=1}^{4}(H_{4n}, H_{5n}) M_n e^{(k_n z + wt + ibx)} + \sum_{n=1}^{4}(H_{4(n+4)}, H_{5(n+4)}) M_{n+4} e^{(-k_n z + wt + ibx)}. \quad (20)$$

$$\sigma_{xz}(z) = \sum_{n=1}^{4} H_{6n} M_n e^{(k_n z + wt + ibx)} + \sum_{n=1}^{4} H_{6(n+4)} M_{n+4} e^{(-k_n z + wt + ibx)} \quad (21)$$

Where the coefficient a_i, δ_i, A, B, C, E, H_{in} and $H_{i(n+4)}$ are given in Appendix 1.

The basic equation in the fluid is given by Othman and Ismail [23]

$$\lambda^f \nabla(\nabla . \boldsymbol{u}^f) = \rho^f \boldsymbol{u}^f_{,tt}, \quad (22)$$

$$\sigma_{ij}^f = \lambda^f u_{r,r}^f \delta_{ij}. \quad (23)$$

Substituting from Eq. (12) into Eq. (22)

$$\left(\frac{w^2}{(c_1^f)^2} - b^2\right) u_1^{*f} + i\, b\, \mathrm{D}\, u_3^{*f} = 0, \quad (24)$$

$$\left(\mathrm{D}^2 + \frac{w^2}{(c_1^f)^2}\right) u_3^{*f} + i\, b\, \mathrm{D}\, u_1^{*f} = 0. \quad (25)$$

Where, $c_1^{f^2} = \dfrac{\lambda^f}{\rho^f}$.

Eliminating u_1^{*f}, u_3^{*f} between Eqs. (24) and (25), we obtain

$$[\mathrm{D}^2 - r^2](u_1^{*f}, u_3^{*f}) = 0. \quad (26)$$

The root of the auxiliary equation of Eq. (26) is $r^2 = (-\frac{w^2}{(c_1^f)^2} + b^2\ )$, and the solution of Eq. (26) has the form

$$(\bar{u}_1^f\ ,\bar{u}_3^f\ )(z) = (1, L_{11}) R_1 e^{rz} + (1, L_{12}) R_2 e^{-rz}\ . \tag{27}$$

Substituting from Eq. (12) in Eq. (23) and by using Eq. (27), we acquire the stress components in a fluid layer.

$$\sigma_{xx}^{*f}(z) = \sigma_{yy}^{*f}(z) = \sigma_{zz}^{*f}(z) = L_{21}\ R_1\ e^{rz} + L_{22}\ R_2\ e^{-rz}. \tag{28}$$

Where, $L_{11} = \dfrac{-i\,b\,r}{[\ r^2 + \frac{w^2}{(c_1^f)^2}\ ]}$, $L_{12} = \dfrac{i\,b\,r}{[\ r^2 + \frac{w^2}{(c_1^f)^2}\ ]}$, $L_{21} = \lambda^f [ib + rL_{11}]$, $L_{22} = \lambda^f [ib - rL_{12}]$.

4. Boundary conditions

To find the constants M_n, M_{n+4}, R_1 and R_2, we have applied boundary conditions for this problem at $z = \pm\, d$,

$$\sigma_{xx} = \sigma_{xx}^f, \quad \sigma_{xz} = f_1\, e^{ib(x-\xi t)}, \quad \frac{\partial u_1}{\partial z} = \frac{\partial u_1^f}{\partial z}, \quad \varphi = 0, \quad T = f_2\, e^{ib(x-\xi t)}. \quad \text{at } z = \pm\, d \tag{29}$$

Using the expressions for $u_1, u_1^f, \sigma_{xx},\ \sigma_{xz}, \sigma_{xx}^f, \varphi,$ and T in (29), we get

$$\sum_{n=1}^{4} H_{4n}\, M_n e^{k_n d} + \sum_{n=1}^{4} H_{4(n+4)} M_{n+4}\ e^{-k_n d} - L_{22} R_2\ e^{-rd} = 0,$$

$$\sum_{n=1}^{4} H_{4n}\, M_n e^{-k_n d} + \sum_{n=1}^{4} H_{4(n+4)} M_{n+4}\ e^{k_n d} - L_{21} R_1\ e^{-rd} = 0,$$

$$\sum_{n=1}^{4} H_{6n}\, M_n e^{k_n d} + \sum_{n=1}^{4} H_{6(n+4)} M_{n+4}\ e^{-k_n d} = f_1,$$

$$\sum_{n=1}^{4} H_{6n}\, M_n e^{-k_n d} + \sum_{n=1}^{4} H_{6(n+4)} M_{n+4}\ e^{k_n d} = f_1,$$

$$\sum_{n=1}^{4} k_n M_n\, e^{k_n d} - \sum_{n=1}^{4} k_n M_{n+4}\, e^{-k_n d} + r\, R_2\, e^{-rd} = 0,$$

$$\sum_{n=1}^{4} k_n M_n\, e^{-k_n d} - \sum_{n=1}^{4} k_n M_{n+4}\, e^{k_n d} - r\, R_1\, e^{-rd} = 0,$$

$$\sum_{n=1}^{4} H_{3n} M_n \, e^{k_n d} + \sum_{n=1}^{4} H_{3(n+4)} M_{n+4} \, e^{-k_n d} = 0,$$

$$\sum_{n=1}^{4} H_{3n} M_n \, e^{-k_n d} + \sum_{n=1}^{4} H_{3(n+4)} M_{n+4} \, e^{k_n d} = 0,$$

$$\sum_{n=1}^{4} H_{2n} M_n \, e^{k_n d} + \sum_{n=1}^{4} H_{2(n+4)} M_{n+4} \, e^{-k_n d} = f_2,$$

$$\sum_{n=1}^{4} H_{2n} M_n \, e^{-k_n d} + \sum_{n=1}^{4} H_{2(n+4)} M_{n+4} \, e^{k_n d} = f_2, \tag{30}$$

By solving the system of non-homogeneous equations (30), the constants M_n, M_{n+4}, R_1 and R_2, can be obtained, then, we define the distribution of all the field quantities.

5. Numerical results and discussion

The analysis is conducted for aluminum epoxy-like material as [24]:

$\beta_0 = \beta_1 = 0,05\times10^5 \; N/m^2.k$, $c_e = 966 \; J/kg.k$, $k = 252 \; J/m.s.k$, $j_0 = 0.196\times10^{-4} \; m^2$,

$\lambda = 7.59\times10^{10} \; N/m^2$, $\mu = 1.89\times10^{10} \; N/m^2$, $a_0 = 0.61\times10^{-10} \; N$, $\rho = 2.19\times10^3 \; kg/m^3$,

$\lambda_0 = \lambda_1 = 0.37\times10^{10} \; N/m^2$, $T_0 = 293k$, $P = 0.001$, $\tau_\theta = 1.5\times10^{-4}$, $\tau_q = 9\times10^{-4}$, $w = w_0 + i\zeta$

, $w_0 = -1.77\times10^{-4}$, $\zeta = 3.59\times10^{-3}$, $b = 3$, $f_1 = 0.025$, $f_2 = 0.025$

As a non-viscous fluid, water has the physical constants are given by Othman and Ismail [23]

$\lambda^f = 2.25\times10^9 \; \mathrm{N.m^{-2}}$, $\rho^f = 10^3 \; \mathrm{kg.m^{-3}}$.

In this paper, the calculations are carried out to a value dimensionless time $t = 1.02$ in the range $-2 \le z \le 2$ on the surface $x = 0.5$. The numerical strategy stated herein is used to distribute horizontal displacement u_1, vertical displacement u_3, temperature T , micro-elongational scalar φ ,stresses components σ_{xx}, σ_{zz}, and σ_{xz} against distance z. To study the effect of the presence and complete absence of gravity in the DPL model and L-S. This paper introduces the results of the numerical assessment in the form of a graph. Fig. 2 presents the variation of the horizontal displacement u_1 as a function of the spatial or temporal variable, comparing two different cases: the presence and the complete absence of gravity. It is evident that gravity has a notable impact on the displacement distribution, leading to either an increase or decrease in displacement depending on the spatial region. The displacement curve under the influence of gravity typically shows steeper gradients and larger amplitudes, highlighting gravity's role in altering wave propagation behavior and influencing the deformation characteristics of the material. Fig. 3 illustrates the variation of the vertical displacement u_3 under two scenarios: with and without gravity. The curves show that gravity affects the magnitude and distribution of vertical displacement through the material. In areas characterized by strong mechanical or thermal gradients, gravity tends to either amplify or diminish the displacement relative to the case without gravitational influence. This behavior underscores the anisotropic nature induced by gravity, which affects the vertical movement of material particles during thermoelastic interactions. Fig. 4 the temperature distribution T is plotted for both the presence and absence of gravity. The curves reveal that the gravity not only affects the mechanical response but also has a noticeable impact on thermal fields. Specifically, temperature diffusion and the resulting thermal gradients are altered in the stressed material. The figure indicates that gravity may either hasten or slow down the thermal response, depending on whether it acts in a compressive or tensile manner, thereby affecting the heat conduction process within the thermoelastic medium. Fig. 5 shows the variation of the micro-elongational scalar φ with and without gravity. The micro-elongation, which represents internal structural deformations at the micro-scale, is significantly influenced by the pre-existing stress state. In the stressed case, φ shows distinct peaks or troughs, indicating enhanced microstructural activity. The comparison suggests that gravity plays a crucial role in micro-mechanical processes and might lead to more complex internal deformation patterns within the material. Fig. 6 shows the force stress component σ_{xx} (normal stress in the x-direction) is plotted for both cases. It is clear from the figure that gravity affects the stress distribution within the material. The stressed configuration exhibits higher peak values and sharper transitions in the stress field compared to the unstressed case. These observations underline how gravity modifies internal forces, potentially leading to different failure modes or stability conditions in thermoelastic bodies. Fig. 7 depicts the variation of the force stress component σ_{zz} (normal stress in the z-direction). Similar to the horizontal stress component, the vertical stress shows distinct differences between the stressed and unstressed states. In the presence of gravity, the material experiences either elevated or reduced stress concentrations depending on the location. The behavior of σ_{zz} reflects how the initial conditions influence vertical load-bearing capacity and mechanical equilibrium. figure, the variation of the force stress component σ_{xz} (shear stress component) is presented. The curves reveal that gravity has a pronounced effect on the distribution of shear stress. The locations of stress concentration or relief vary notably between scenarios with and without gravity, reflecting the intricate interaction between gravitational forces and thermoelastic shear behavior. The shear stress component shows heightened sensitivity to gravity, emphasizing its influence on the development of shear instabilities or the formation of potential slip zones within the material.

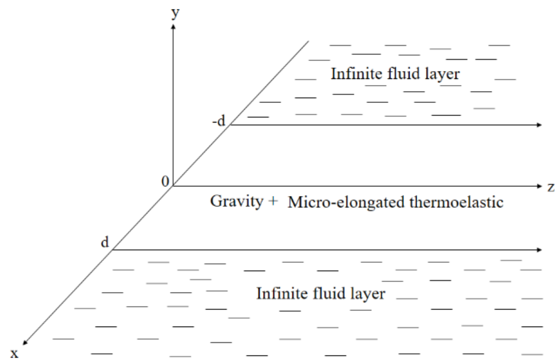

Fig. 1 Geometry of the problem

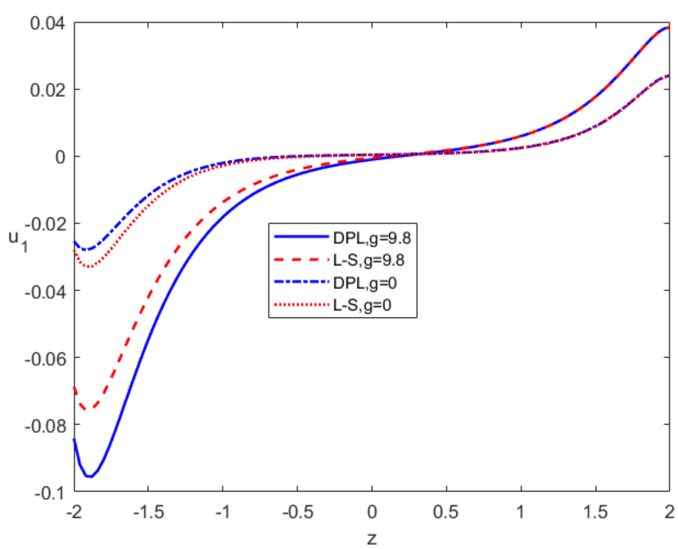

Fig. 2 Variation of the horizontal displacement u_1 in the presence and complete absence of gravity.

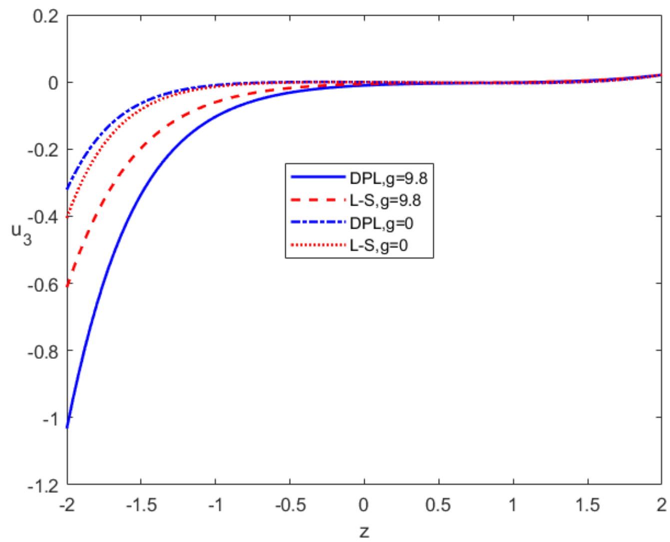

Fig. 3 variation of the vertical displacement u_3 in the presence and complete absence of gravity.

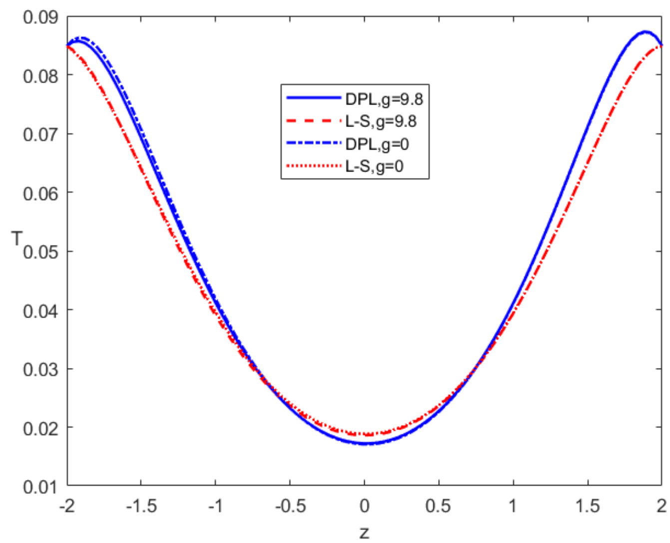

Fig. 4 variation of the temperature T in the presence and complete absence of gravity.

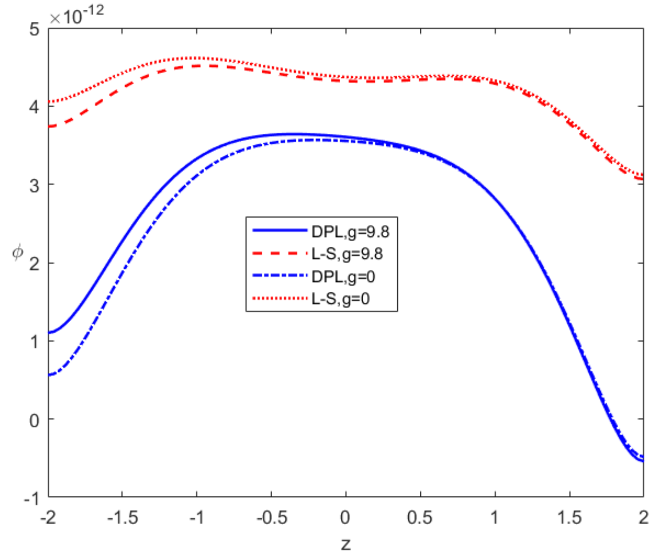

Fig. 5 Variation of the micro-elongational scalar φ in the presence and complete absence of gravity.

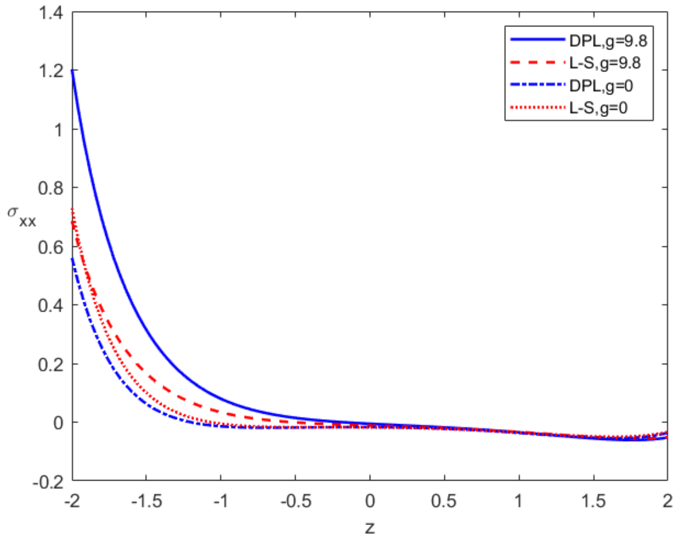

Fig. 6 Variation of the force stress components σ_{xx} in the presence and complete absence of gravity.

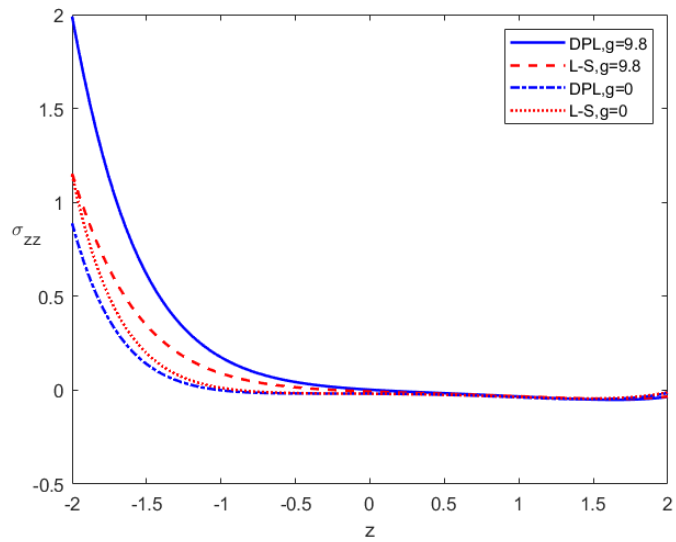

Fig. 7 Variation of the force stress components σ_{zz} in the presence and complete absence of gravity.

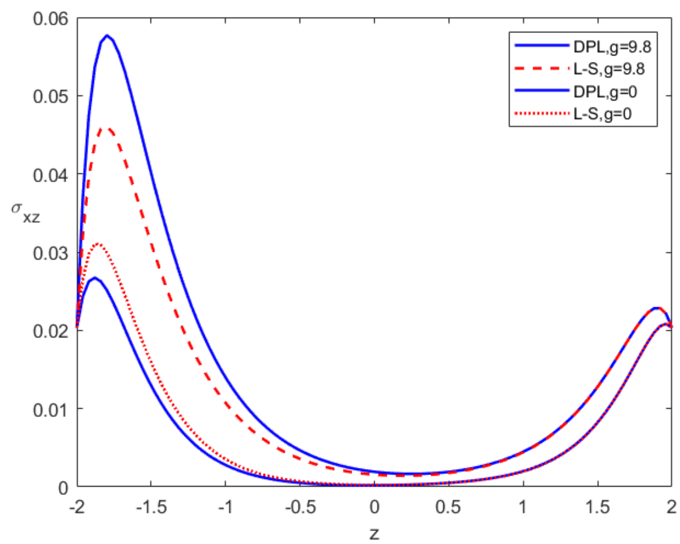

Fig. 8 Variation of the force stress components σ_{xz} in the presence and complete absence of gravity.

6. Conclusion

This work presents a detailed analytical study exploring the impact of gravity on a micro-elongated thermoelastic half-space immersed in an infinitely extending inviscid fluid, using both the Dual-DPL model and L-S theory. The investigation begins with the derivation of the governing equations, which are then non-dimensionalized and simplified using normal mode analysis. This approach transforms the original system of partial differential equations into a more tractable set of ordinary differential equations. Gravity is explicitly incorporated into the formulation, and appropriate boundary conditions are applied at the interface to determine the integration constants. Numerical simulations are carried out to illustrate and compare the behavior of key physical quantities—such as displacement, temperature, and stress—both with and without the influence of gravity. The findings highlight that gravity significantly affects the thermoelastic and microstructural behavior of the medium. Under both the DPL and L-S frameworks, gravity modifies the amplitude, phase, and propagation characteristics of thermal and mechanical waves. Additionally, comparisons between the two models show that the DPL theory, which accounts for phase-lag effects, offers a more refined representation of the system, particularly in capturing the finite speed of thermal signals and the delayed interactions between thermal and mechanical fields.

List of symbols

ρ	Density in micro-elongated medium
σ_{ij}	Component of stress tensor for micro-elongated medium
u	Displacement vector in micro-elongated medium
$a_0, \lambda_0, \lambda_1$	Micro-elongational constants
g	gravity
j_0	Microinertia
$\alpha_{t_1}, \alpha_{t_2}$	Coefficient of linear thermal expansion where $\beta_0 = (3+2\mu)\alpha_{t_1}, \beta_1 = (3+2\mu)\alpha_{t_2}$
φ	Micro-elongational scalar
T_0	Reference temperature
T	Absolute temperature
c_e	Specific heat at the constant strain in micro-elongated medium

k Thermal conductivity in micro-elongated medium

τ_θ Temperature gradient parameter

τ_q Heat flux parameter

λ, μ Lame's constants in micro-elongated medium

λ^f Bulk modulus

$\boldsymbol{u}^f$ Displacement vector for fluid

σ_{ij}^f Component of stress tensor of fluid

ρ^f Density of fluid

c_1^f Velocity of sound of fluid

References

[1] Biot M.A., Thermoelasticity and irreversible thermodynamics. Journal of applied physics, 1956. 27(3) 240-253.

[2] Lord H.W. and Shulman Y., A generalized dynamical theory of thermoelasticity. Journal of the Mechanics and Physics of Solids, 1967. 15(5) 299-309.

[3] Green A.E. and Lindsay K.A., Thermoelasticity. Journal of Elasticity, 1972. 2(1) 1-7.

[4] Green A.E. and Naghdi P.M., A re-examination of the basic postulates of thermomechanics. roceedings of the Royal Society of London. Series A: Mathematical and Physical Sciences, 1991. 32(1885) 171-194.

[5] Green A.E. and Naghdi P.M., On undamped heat waves in an elastic solid. Journal of Thermal Stresses, 1992. 15(2) 253-264.

[6] Green A.E. and Naghdi P.M., Thermoelasticity without energy dissipation. Journal of Elasticity, 1993. 31(3) 189-208.

[7] Othman M.I.A. and Tantawi R.S., The effect of a laser pulse and gravity field on a thermoelastic medium under Green–Naghdi theory. Journal of Acta Mechanica, 1993. 227(12) 3571-3583.

[8] Othman M.I.A. and Atwa S.Y., Response of micropolar thermoelastic solid with voids due to various sources under Green Naghdi theory. Journal of Acta Mechanica Solida Sinica. 2012. 25(2) 197-209.

[9] Tzou D.Y., A Unified Field Approach for Heat Conduction From Macro- to Micro-Scales. Journal of Heat Transfer, 1995. 117(1) 8-16.

[10] Tzou D.Y., The generalized lagging response in small-scale and high-rate heating. International Journal of Heat and Mass Transfer, 1995. 38(17) 3231-3240.

[11] Said, S. M., Influence of gravity on generalized magneto-thermoelastic medium for three-phase-lag model. Journal of Computational and Applied Mathematics, 2016. 291, 142-157.

[12] Eringen A., Linear theory of micropolar elasticity", ONR Technical Report No. 29, School of Aeronautics, Aeronautics and Engineering Science, Purdue University, West Lafayette, IN. 1965, Purdue University.

[13] Eringen A.C., A unified theory of thermomechanical materials. International Journal of Engineering Science, 1966. 4(2) 179-202.

[14] Eringen A.C., Linear theory of micropolar elasticity. Journal of Mathematics and Mechanics, 1966. 15(6) 909-923

[15] Eringen A.C., Theory of thermo-microstretch elastic solids. International Journal of Engineering cience, 1990. 28(12) 1291-1301.

[16] Shaw S. and Mukhopadhyay B., Periodically varying heat source response in a functionally graded microelongated medium. Applied Mathematics and Computation, 2012. 218(11) 6304-6313.

[17] Shaw S. and Mukhopadhyay B., Moving heat source response in a thermoelastic microelongated Solid. Journal of Engineering Physics and Thermophysics, 2013. 86(3) 716-722.

[18] Ailawalia P., Sachdeva S.K. , and Pathania D.S., Plane strain deformation in a thermoelastic microelongated solid with Internal heat source. International Journal of Applied Mechanics and Engineering, 2015. 20(4) 717-731.

[19] Sachdeva S.K. and Ailawalia P., Plane strain deformation in thermoelastic microelongated solid. Civil and Environmental Research, 2015. 7(2) 92-98.

[20] Ailawalia P., Kumar S. and Pathania D.S., Internal heat source in thermoelastic microelongated solid under green lindsay theory. Journal of Theoretical and Applied Mechanics, 2016. 46(2) 65-82.

[21] Abo-Dahab S. M., Bayones F. S., Alharbi F. M., Abd-Alla A. M., Aljohani A. F., and Kilany A. A., Magneto-thermoelastic surface waves phenomenon with voids, gravity, initial stress, and rotation under four theories. Alexandria Engineering Journal, 2024. 105, 743-759..

[22] Ahmed E.A., Abou-Dina M.S. and El Dhaba A.R., Effect of gravity on piezo-thermoelasticity within the dual-phase-lag model. Journal of Microsystem Technologies, 2019. 25(1) 1-10.

[23] Othman M. I. A. and Ismail M. F., The gravitational field effect on a micro-elongated thermoelastic layer under a fluid load with two theories. Multidiscipline Modeling in Materials and Structures, 2022. 18(5), 757-771.

[24] Shaw S. and Mukhopadhyay B., Moving heat source response in a thermoelastic microelongated Solid. Journal of Engineering Physics and Thermophysics, 2013. 86(3) 716-722.

Appendix 1

$$a_1 = \frac{\mu}{\rho c_1^2},\ a_2 = \frac{\lambda+\mu}{\rho c_1^2},\ a_3 = \frac{\beta_1 \lambda_0 c_1^2}{a_0 \beta_0 w^{*2}},\ a_4 = \frac{\lambda_1 c_1^2}{a_0 w^{*2}},\ a_5 = \frac{\lambda_0^2}{a_0 \rho w^{*2}},\ a_6 = \frac{\rho j_0 c_1^2}{2a_0},\ a_7 = \frac{\rho c_e c_1^2}{k w^*},\ a_8 = \frac{\beta_0^2 T_0}{k \rho w^*},$$

$$a_9 = \frac{\beta_0 \beta_1 T_0 c_1^2}{k \lambda_0 w^*},\quad a_{10} = \frac{\lambda}{\rho c_1^2},\quad \delta_1 = a_1 b^2 + a_2 b^2 + w^2,\quad \delta_2 = iba_2,\ \delta_3 = a_1 + a_2,\quad \delta_4 = a_1 b^2 + +w^2,\quad \delta_5 = iba_5,$$

$$\delta_6 = b^2 + +a_4 + a_6 w^2,\ \delta_7 = 1 + \tau_\theta w,\ \delta_8 = 1 + \tau_q w,\ \delta_9 = iba_8 w \delta_8,\ \delta_{10} = a_8 w \delta_8,\ \delta_{11} = b^2 \delta_7 + a_7 w \delta_8,$$

$$\delta_{12} = a_9 w,$$

$$A = \frac{-1}{a_1 \delta_3 \delta_7}[-\delta_2^2 \delta_7 - a_1 \delta_{10} + a_1 a_5 \delta_7 - a_1 \delta_4 \delta_7 - a_1 \delta_3 \delta_{11} - \delta_1 \delta_3 \delta_7 - a_1 \delta_3 \delta_6 \delta_7],$$

$$\begin{aligned} B = \frac{1}{a_1 \delta_3 \delta_7}[&\delta_2^2 \delta_{11} + \delta_1 \delta_{10} + \delta_2 \delta_9 - a_1 a_3 \delta_{10} - a_1 a_5 \delta_{11} - a_1 a_5 \delta_{12} - a_5 \delta_1 \delta_7 + a_1 \delta_4 \delta_{11} + a_1 \delta_6 \delta_{10} + ib \delta_2 \delta_{10} - ib \delta_3 \delta_9 \\ &+ \delta_1 \delta_4 \delta_7 - \delta_2 \delta_5 \delta_7 + \delta_1 \delta_3 \delta_{11} + \delta_2^2 \delta_6 \delta_7 - b^2 g^2 \delta_7 + a_1 a_3 \delta_3 \delta_{12} - ia_5 b \delta_2 \delta_7 + a_1 \delta_4 \delta_6 \delta_7 + a_1 \delta_3 \delta_6 \delta_{11} \\ &+ ib \delta_3 \delta_5 \delta_7 + \delta_1 \delta_3 \delta_6 \delta_7] \end{aligned}$$

$$\begin{aligned} C = \frac{-1}{a_1 \delta_3 \delta_7}[&a_3 \delta_1 \delta_{10} + a_3 \delta_2 \delta_9 + a_5 \delta_1 \delta_{11} + a_5 \delta_1 \delta_{12} - a_3 \delta_2^2 \delta_{12} + ib \delta_4 \delta_9 - \delta_1 \delta_4 \delta_{11} - \delta_1 \delta_6 \delta_{10} - \delta_2 \delta_6 \delta_9 + \delta_2 \delta_5 \delta_{11} \\ &+ \delta_2 \delta_5 \delta_{12} - \delta_2^2 \delta_6 \delta_{11} + b^2 g^2 \delta_{11} + b^2 g^2 \delta_6 \delta_7 - a_1 a_3 \delta_4 \delta_{12} + iba_3 \delta_2 \delta_{10} - iba_3 \delta_3 \delta_9 + iba_5 \delta_2 \delta_{11} + iba_5 \delta_2 \delta_{12} \\ &- a_3 \delta_1 \delta_3 \delta_{12} - a_1 \delta_4 \delta_6 \delta_{11} - ib \delta_4 \delta_5 \delta_7 - ib \delta_2 \delta_6 \delta_{10} + ib \delta_3 \delta_6 \delta_9 - ib \delta_3 \delta_5 \delta_{11} - ib \delta_3 \delta_5 \delta_{12} - \delta_1 \delta_4 \delta_6 \delta_7 - \delta_1 \delta_3 \delta_6 \delta_{11}], \end{aligned}$$

$$E = \frac{1}{a_1 \delta_3 \delta_7}[iba_3 \delta_4 \delta_9 + a_3 \delta_1 \delta_4 \delta_{12} - ib \delta_4 \delta_6 \delta_9 + ib \delta_4 \delta_5 \delta_{11} + ib \delta_4 \delta_5 \delta_{12} + \delta_1 \delta_4 \delta_6 \delta_{11} - a_3 b^2 g^2 \delta_{12} - b^2 g^2 \delta_6 \delta_{11}]$$

$$H_{1n} = H_{1(n+4)} = \frac{k_n \delta_2 + ibk_n \delta_3 - \delta_1 k_n^3}{(ib\delta_4 - \delta_3) k_n^2 - ib\delta_5},\ H_{2n} = H_{2(n+4)} = \frac{k_n^3 \delta_{11} H_{1n} + a_5 \delta_{11} k_n H_{1n} + \delta_7 \delta_{11} H_{1n} k_n - k_n^2 \delta_{10} - \delta_6 \delta_{13} + \delta_7 \delta_{10}}{\delta_7 \delta_8 k_n^2 + \delta_{12} k_n^2 - \delta_8 k_n^4 - \delta_7 \delta_{12} - a_3 \delta_{12}},$$

$$H_{3n} = H_{3(n+4)} = \frac{a_5 k_n H_{1n} + a_3 H_{2n} - \delta_6}{\delta_7 - k_n^2},\quad H_{4n} = H_{4(n+4)} = ib - a_{10} k_n H_{1n} - H_{2n} + H_{3n},\quad H_{5n} = H_{5(n+4)} = iba_{10} - k_n H_{1n} - H_{2n} + H_{3n},$$

$$H_{6n} = H_{6(n+4)} = iba_{13} H_{1n} - a_{12} k_n.$$